Continuum model for polymers with finite thickness

2005 J. Phys. A: Math. Gen. 38 L277

(http://iopscience.iop.org/0305-4470/38/17/L01)

INSTITUTE OF PHYSICS PUBLISHING JOURNAL OF PHYSICS A: MATHEMATICAL AND GENERAL

J. Phys. A: Math. Gen. **38** (2005) L277–L283 doi:10.1088/0305-4470/38/17/L01

LETTER TO THE EDITOR

Continuum model for polymers with finite thickness

D Marenduzzo[1,2], C Micheletti[3], H Seyed-allaei[3], A Trovato[4] and A Maritan[4]

[1] Department of Physics, Theoretical Physics, University of Oxford, 1 Keble Road, Oxford OX1 3NP, UK
[2] Mathematics Institute, University of Warwick, CV4 7AL, UK
[3] International School for Advanced Studies (SISSA) and INFM, Via Beirut 2-4, 34014 Trieste, Italy
[4] INFM and Dip. di Fisica 'G. Galilei', Universitá di Padova, Via Marzolo 8, 35131 Padova, Italy

Received 11 March 2005
Published 13 April 2005
Online at stacks.iop.org/JPhysA/38/L277

Abstract

We consider the continuum limit of a recently introduced model for discretized thick polymers, or tubes. We address both analytically and numerically how the polymer thickness influences the decay of tangent–tangent correlations and find how the persistence length scales with the thickness and the torsional rigidity of the tube centreline. At variance with the worm-like chain model, the phase diagram that we obtain for a continuous tube is richer; in particular, for a given polymer thickness there exists a threshold value for the centreline torsional rigidity separating a simple exponential decay of the tangent–tangent correlation from an oscillatory one.

PACS numbers: 82.35.Lr, 87.15.−v, 36.20.Ey

Experimental studies of biopolymers have constantly stimulated the search for schematic models apt for reproducing the observed kinetic and thermodynamic behaviour. In recent years, two types of biopolymers have attracted most of these efforts: DNA and proteins. The interest in the former has been sparked by the introduction of single-molecule experiments which probed the elastic response of DNA upon stretching [1]. Considerable progress in the rationalization of these experiments was made thanks to the worm-like chain (WLC) model [2, 3] where the polymer is described as a continuous centreline possessing an effective bending [2] and/or twisting [4, 5] rigidity. For protein modelling, instead, one of the goals is to capture the main physico-chemical forces responsible for driving the folding process towards the native state. Typical coarse-grained models adopt sophisticated energy functionals (often with hundreds of parameters) in order to reproduce the observed variety of protein folds. It has been recently argued, however, that the overburdening of the energy function can be avoided by modelling explicitly the intrinsic thickness of proteins [6–9]. As we discuss later, this is achieved through the introduction of suitable three-body interactions among triplets of points constituting the polymer centreline [8, 10–13]. It is physically appealing that the

thick-chain model has proved valuable also for the case of DNA in applications ranging from the characterization of knotted DNA molecules [14] to the thermodynamics of DNA packaging inside viral capsids and DNA elastic response [15].

By necessity, all numerical implementations of these models rely on the discretization of the polymer centreline into a succession of beads whose 'natural' spacing is typically suggested by the intrinsic granularity of the polymer itself (e.g. the separation of consecutive C_αs for proteins or the base-pair spacing in dsDNA). From a theoretical perspective, it is therefore desirable to characterize the thick-chain model in the continuum limit, where the bead spacing tends to zero (analogously to the WLC limit of the Kratky–Porod model). This continuum limit has, so far, been considered only for characterizing the limited repertoire of ideal knots. Motivated by the potentially wide range of applicability of the thick-polymer model, in this letter we take the perspective of addressing the statistical mechanics of generalized thick-polymer models in the continuum limit. In particular, we introduce in the Hamiltonian a penalty for the geometrical torsion of the tube centreline and, initially, consider the constraints induced by the finite polymer thickness only at a local level, a simplification usually adopted to allow analytical progress [4, 5]. From the exact analysis, it emerges that accounting for the centreline torsional rigidity term (1) allows us to get a finite persistence length in the limit of a continuous thick polymer and (2) introduces a novel feature in the behaviour of the tangent–tangent correlation function, namely the presence of a threshold value for the torsional rigidity which separates a monotonic decay from an oscillatory one. Finally, numerical Monte Carlo simulations are employed to show that this behaviour persists also when the tube constraint is enforced at non-local level. These findings highlight the rich behaviour of models where the thickness is treated explicitly. As a comparison, we consider the case of a WLC in the presence of penalty for the centreline geometrical torsion. It is found that this model exhibits *either* a simple exponential decay *or* an oscillatory one (with singular behaviour in the continuum limit) depending, respectively, on the absence or presence of the torsional rigidity but independently of its strength. In relation to the behaviour observed here, it should also be noted that Panyukov and Rabin [16] have considered a rod-like chain fluctuating around a stress-free helical conformation. Under these conditions they could observe a change from an oscillatory to a simple exponential decay by increasing the fluctuation strength.

We model a polymer chain by means of a set of N consecutive beads, $\{\vec{r}_0 \dots \vec{r}_{N-1}\}$ connected by bonds of fixed length, a. The succession of beads constitutes the centreline for our thick polymer. We shall denote by Δ and κ_t the thickness of the chain and the torsional rigidity, respectively. Although we shall first focus on the case $\kappa_t = 0$ we will develop a formalism general enough to be used also in the WLC with torsional penalty. By analogy with the Frenet reference frame for continuous curves [17], we define an orthonormal set associated with each bead, formed by the local *tangent*, $\hat{t}_i \equiv (\vec{r}_{i+1} - \vec{r}_i)/a$, *binormal*, $\hat{b}_i \equiv \hat{t}_i \wedge \hat{t}_{i-1}/|\hat{t}_i \wedge \hat{t}_{i-1}|$ and '*normal*', $\hat{n}_i \equiv \hat{t}_i \wedge \hat{b}_i$ (see figure 1(*a*), note that in the usual definition of the Frenet triad the normal has the opposite sign). It is possible to write recursion equations relating the reference axes for bead i in terms of those for bead $i-1$, using the polar angles θ_i and ϕ_i as in figure 1(*b*):

$$\begin{cases} \hat{b}_i = \cos\phi_i \hat{b}_{i-1} - \sin\phi_i \hat{n}_{i-1}, \\ \hat{t}_i = \sin\theta_i \sin\phi_i \hat{b}_{i-1} + \cos\theta_i \hat{t}_{i-1} + \sin\theta_i \cos\phi_i \hat{n}_{i-1}, \\ \hat{n}_i = \cos\theta_i \sin\phi_i \hat{b}_{i-1} - \sin\theta_i \hat{t}_{i-1} + \cos\theta_i \cos\phi_i \hat{n}_{i-1}. \end{cases}$$

Quite generally the joint probability distribution of angles, $\mathcal{P}(\theta_1, \theta_2, \phi_2, \theta_3, \phi_3, \dots)$, resulting from the canonical average, will depend on the whole ensemble of interactions including the steric ones. However, for the simplified case where the effects of the polymer thickness

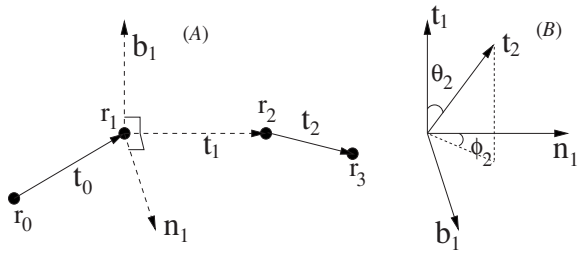

Figure 1. Frenet reference frame for a discrete bead model. Note that $\theta_i \in [0, \pi]$ is defined for $1 \leqslant i \leqslant N-2$, whereas $\phi_i \in [0, 2\pi]$ is defined only for $2 \leqslant i \leqslant N-2$.

are treated only locally (as for twist and bending rigidity) then $\mathcal{P}$ factorizes in terms of the probability distributions $\rho(\theta_i, \phi_i)$ for each pair of angles θ_i, ϕ_i:

$$\mathcal{P}(\theta_1, \phi_2, \theta_2, \phi_3, \theta_3, \ldots) = \rho_\theta(\theta_1) \prod_{i=2}^{N-2} \rho(\theta_i, \phi_i). \tag{1}$$

Since we are considering a uniformly thick homopolymer, the same probability distribution, $\rho(\theta, \phi)$, is involved for all beads. In the following, the averages weighted with ρ will be denoted as $\langle\cdot\rangle$, while those calculated with respect to $\mathcal{P}$ will be written as $\langle\cdot\rangle_{\mathcal{P}}$. The factorization leads to a straightforward characterization of the decay along the chain of expectation values such as $f_i \equiv \langle \hat{b}_i \cdot \vec{x}\rangle_{\mathcal{P}}$, $g_i \equiv \langle \hat{t}_i \cdot \vec{x}\rangle_{\mathcal{P}}$, $h_i \equiv \langle \hat{n}_i \cdot \vec{x}\rangle_{\mathcal{P}}$, where $\vec{x}$ could be, e.g., $\hat{t}_1, \hat{b}_1, \hat{n}_1$. In fact, f, g and h at location $i+1$ are obtained from those at site i by the application of the following transfer matrix:

$$\mathbf{T} = \begin{pmatrix} \langle\cos\phi\rangle & 0 & -\langle\sin\phi\rangle \\ \langle\sin\theta\sin\phi\rangle & \langle\cos\theta\rangle & \langle\sin\theta\cos\phi\rangle \\ \langle\cos\theta\sin\phi\rangle & -\langle\sin\theta\rangle & \langle\cos\theta\cos\phi\rangle \end{pmatrix}. \tag{2}$$

If the eigenvalues of $\mathbf{T}$ are real, the decay of f, g and h will be monotonic, while if they are imaginary there will be an oscillatory modulation.

We now consider two further simplifying assumptions: (i) the 'bond' angle θ and the 'dihedral' angle ϕ contribute independently to the probability distribution $\rho(\theta, \phi) = \rho_\theta(\theta)\rho_\phi(\phi)$, and (ii) the system is invariant for chirality flipping $\rho_\phi(\phi) = \rho_\phi(-\phi)$. In this case, $\langle\sin\phi\rangle = 0$, and the transfer matrix $\mathbf{T}$ becomes block diagonal with an eigenvalue $\lambda_1 = \langle\cos\phi\rangle$, so that $\langle \hat{b}_n \cdot \hat{b}_1\rangle = \lambda_1^{n-1} = \exp[-a(n-1)/\xi_b]$ decays exponentially with a correlation length $\xi_b = -a/\ln\langle\cos\phi\rangle$. The remaining two eigenvalues are the solutions of the second-order equation $\lambda^2 - b\lambda + c = 0$ with $b = \langle\cos\theta\rangle[1 + \langle\cos\phi\rangle]$, $c = \langle\cos\phi\rangle[\langle\cos\theta\rangle^2 + \langle\sin\theta\rangle^2]$. The relevant quantity which discriminates between different decay properties is $\Gamma \equiv b^2 - 4c$. If $\Gamma > 0$, the two solutions $\lambda_{2,3} = (\pm\sqrt{\Gamma} + b)/2$ are real and the correlation function for tangent/normal vectors decays exponentially to zero, with the correlation length $\xi_t = -a/\ln\lambda_2$ being controlled by the largest eigenvalue. If $\Gamma < 0$, the two solutions are complex conjugate, and the tangent–tangent correlation function exhibits an oscillatory decay:

$$\langle \hat{t}_{n+1} \cdot \hat{t}_1\rangle = \frac{\cos[a/\chi_0 + an/\chi]}{\cos\chi_0}\, \mathrm{e}^{-an/\xi_t}, \tag{3}$$

where $\xi_t = -2a/\ln c$, $\chi = a/\arctan(\sqrt{-\Gamma}/b)$, and χ_0 depends on initial conditions.

Within this general framework, we now consider different specific examples. We first focus on the case of a WLC subject to a penalty for the geometrical torsion; the corresponding

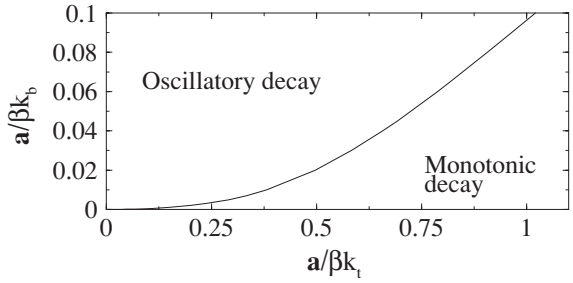

Figure 2. Boundary separating the oscillatory from the exponential decay of the tangent–tangent correlation.

Hamiltonian is

$$\mathcal{H}_{\mathrm{WLC}} = \frac{\kappa_b}{2a}\sum_i |\hat{t}_{i+1} - \hat{t}_i|^2 + \frac{\kappa_t}{2a}\sum_i |\hat{b}_{i+1} - \hat{b}_i|^2, \tag{4}$$

where κ_b, κ_t, are the bending and torsional rigidity, respectively, defined in such a way to get back the usual Hamiltonian in the continuous limit, $a \to 0$. We emphasize the fact that the Hamiltonian (4) is entirely specified by the centreline geometry. The approach therefore differs in spirit from those used to model the elasticity of rod-like chains. In these contexts, starting from a stress-free reference configuration, one introduces a 'material reference frame' which is used to keep track not only of the deformations of a given reference frame, but also of the twist around the centreline [17]. Although this latter information is clearly not available in the model of equation (4) it is worth considering energy functions relying uniquely on the knowledge of the centreline. In fact, for the important class of biopolymers constituted by proteins, it is well known that the knowledge of a protein's centreline (the C_α trace) and sequence composition allows us to reconstruct the whole protein structure with high accuracy.

For the case of Hamiltonian (4), the probability distributions for bond and dihedral angles taking, of course, into account the inverse temperature β are found to be $\rho_\theta(\theta) = \sin\theta \exp\left[\beta\frac{\kappa_b}{a}\cos\theta\right]$; $\rho_\phi(\phi) = \exp\left[\beta\frac{\kappa_t}{a}\cos\phi\right]$. All averages appearing in the transfer matrix elements of equation (2) can formally be expressed by means of modified Bessel functions which, in turn, allow us to identify the boundary, $\Gamma = 0$, separating the oscillatory from the monotonic decay of tangent correlations, see figure 2. In the continuum limit, $a \to 0$, the angles θ and ϕ contributing significantly to the average come from a region centred around zero and of widths $\sqrt{a/\beta\kappa_b}$ and $\sqrt{a/\beta\kappa_t}$, respectively and the equation for the boundary is $a/\beta\kappa_b \approx (a/\beta\kappa_t)^2/8\pi$. This implies that, for any finite value of the torsional rigidity, in the continuum limit the tangent–tangent correlation function always decays in an oscillatory way. The period of the oscillation is proportional to $\sqrt{a\kappa_b}$ while the decay length, ξ_t, is independent of a, $\xi_t^{-1} = 1/(4\beta\kappa_t) + (1 - \pi/4)/(\beta\kappa_b)$. It is therefore apparent that in the continuum limit, $a \to 0$, the oscillation period becomes smaller and smaller, denoting a singular behaviour of the chain. This is reminiscent of the singular behaviour of rod-like chains which, in the continuum limit, exhibit plectonemes on smaller and smaller scales [4, 5]. From figure 2, it is apparent that only if κ_t is exactly zero, one remains in the vanishingly small region of monotonic exponential decay when the continuum limit is taken. In this case one recovers the WLC case with persistence length $\xi_t \sim \beta\kappa_b$. We now consider the case of a polymer chain describing a thick self-avoiding tube of uniform cross-section. The finite thickness Δ of the polymer impacts on two distinct conformational features. First, it constrains the local radius of curvature to be not less than Δ [10, 11]. In addition, there is also a non-local effect since any two portions of the tube, at a finite arclength separation, cannot interpenetrate

[10, 11]. In traditional beads-and-strings models it is only this second effect that is taken into account through a pairwise potential with a hard-core repulsion. Interestingly, one needs to go beyond pairwise interactions to account for the above-mentioned effects in discretized polymer chains [7, 8, 12, 13]. In fact, the requirement on the local radius of curvature can be enforced by finding the radii of the circles going through any consecutive triplet of points and ensuring that each of them is greater than Δ. The non-local effect can be addressed within the same framework by considering the minimum radius among circles going through any non-consecutive triplet of points is also greater than Δ. In summary the finite thickness, Δ, of the discretized tube requires that the radii of the circles going through any triplet of distinct points have to be greater than Δ (see figure 3) [11–13]. In the present context, we are interested mainly in the local thickness effects. Therefore, we will consider the following reduced Hamiltonian in the absence of torsional rigidity, involving only local three-body constraints: $\mathcal{H}_1 = \sum_i V(R_{i-1,i,i+1})$, where R_{ijk} is the radius of the circle going through the beads i, j, k, and the potential $V(R)$ is ∞, if $R < \Delta$, and 0 otherwise. From simple geometric considerations, the local tube constraint can be expressed in terms of the bond angle distribution by imposing $\rho_\theta(\theta_i) = 0$ if $\theta_i > 2\arcsin(a/2\Delta)$. One can see that the thickness Δ plays a role similar to the bending rigidity κ_b, in that they both induce the chain to be locally more straight. Yet, the scaling behaviour in the $a \to 0$ limit is different in the tube case, since the range of θ angles most contributing to the average has now width a/Δ (instead of $\sqrt{a/\beta\kappa_b}$), yielding $\langle\cos\theta\rangle = 1 - a^2/4\Delta^2$ and $\langle\sin\theta\rangle \sim 2a/3\Delta$. Since $\Gamma = \langle\cos\theta\rangle^2 \sim 1 - a^2/2\Delta^2$, the tangent–tangent correlation function decays exponentially. This is similar to the WLC case in the absence of torsional rigidity, but in the tube model the correlation length scales in a different way $\xi_t \sim \Delta^2/a$. This is a pathological behaviour in the continuous limit, since the correlation length diverges as $a \to 0$. The recipe by which the tube constraint is implemented for a discrete chain ends up in preferentially sampling straight continuous lines. It is natural to associate such ill behaviour with the degeneracy in the choice of the Frenet frame which arises for a straight line conformation[5]. This can in fact be cured by adding a torsional rigidity term to the tube constraint, constraining the unphysical fluctuations of the binormal vectors around straight line conformations. The Hamiltonian for this rod-like thick polymer is

$$\mathcal{H}_2 = \sum_i V(R_{i-1,i,i+1}) + \frac{\kappa_t}{2a}\sum_i |\hat{b}_{i+1} - \hat{b}_i|^2. \tag{5}$$

In this case, $\langle\cos\phi\rangle \sim 1 - a/2\beta\kappa_t$ in the $a \to 0$ limit, which implies $\xi_b = 2\beta\kappa_t$ whereas we get $\Gamma \sim \left(a^2/36\beta^2\kappa_t^2\Delta^2\right)\left[9\Delta^2 - 64\beta^2\kappa_t^2\right]$. Thus, there are two different regimes, oscillatory decay if $\kappa_t > \kappa_t^* \equiv \frac{3}{8}\Delta/\beta$, and monotonic decay if $\kappa_t < \kappa_t^*$. In the latter case, the persistence length associated with the tangent–tangent correlation function is controlled by *both* the tube thickness and the torsional rigidity:

$$\xi_t = \frac{9\Delta^2}{16\beta\kappa_t}\left[1 + \sqrt{1 - \left(\frac{8\beta\kappa_t}{3\Delta}\right)^2}\right]. \tag{6}$$

In the former case, the correlation length depends instead only on the torsional rigidity, whereas the oscillation period depends also on the tube thickness:

$$\xi_t = 4\beta\kappa_t, \qquad \chi = \frac{3\Delta}{2}\left[1 - \left(\frac{3\Delta}{8\beta\kappa_t}\right)^2\right]^{-1/2}. \tag{7}$$

[5] A differentiable curve, $\vec{r}(s)$, s being the arclength parametrization, with thickness not smaller than Δ satisfies: $\sup_{s_1,s_2}|\vec{r}(s_1) - \vec{r}(s_2)|/|s_1 - s_2| \leqslant \Delta^{-1}$ [18]. The set of curves satisfying this bound has zero Wiener measure if the latter includes only terms up to the second derivative in $\vec{r}(s)$ [19]. Thus, higher-order derivatives are required for suitable measures of tubes in the continuum limit.

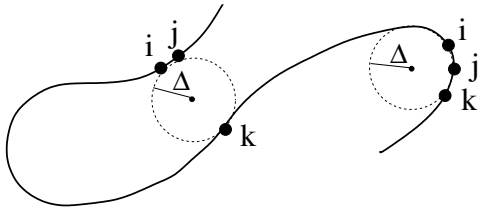

Figure 3. Sketch of a curve which is a viable centreline for a tube of thickness Δ. The radii of the circles through any triplet of points, r_{ijk} are not smaller than Δ.

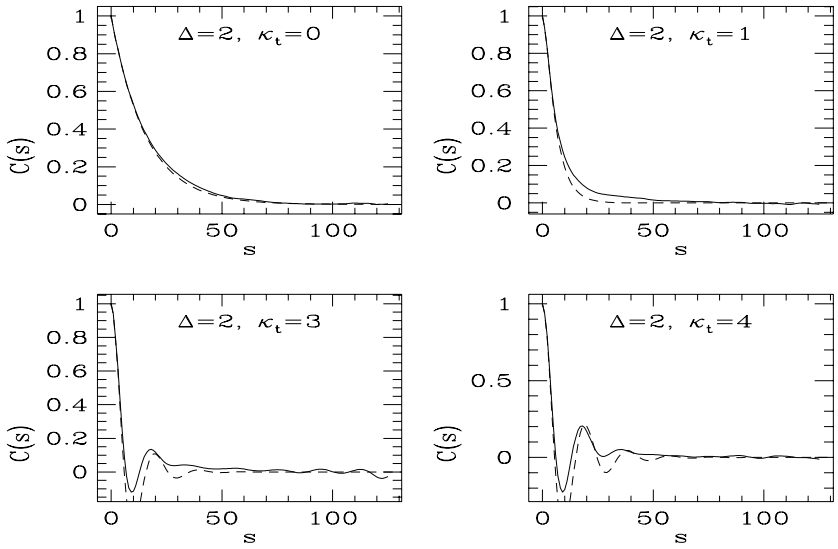

Figure 4. Tangent–tangent correlation, $C(s)$, as a function of the arclength separation, s. The dashed and solid lines refer respectively to the analytical results from equation (2) and to the MC simulations (maximum dispersion ≈0.01).

It can be seen from equation (6), that by increasing the torsional rigidity the tangent–tangent correlation length ξ_t, initially controlled by the thickness Δ decreases until the threshold κ_t^* is reached. Above such a threshold torsional rigidity takes over and the tangent–tangent correlation length becomes equal to twice the binormal–binormal correlation length, but the thickness signature remains in the oscillatory behaviour of the tangent–tangent correlation function and in the period χ. The previous analysis is in good semi-quantitative agreement with data from MC simulations on the full model (i.e. where non-local effects are retained), as visible in figure 4. The simulations were performed on chains of 128 equispaced beads through the Metropolis acceptance of crankshaft and pivot moves. The tangent–tangent correlations were measured by sampling structures at intervals greater than the autocorrelation time.

To conclude, we have shown how the recently introduced thick-polymer model can be regularized in the continuum limit by introducing a term penalizing the geometrical torsion of the centreline. For any given value of the polymer thickness, there exists a torsional-rigidity threshold separating the monotonic decay of the tangent–tangent correlation from the oscillatory one. This highlights the rich behaviour of thick-polymer models which combine features previously observed in distinct polymer models, such as the worm- or rod-like chains. The wide use of the latter in the context of single-molecule experiments opens the possibility

to use the physically appealing perspective of semi-flexible thick polymers to interpret the behaviour of biopolymers.

Acknowledgments

We thank J R Banavar, T X Hoang and F Seno for useful discussions and acknowledge support from COFIN MURST 2003, FISR 2001, INFM and EPSRC.

References

[1] Bustamante C, Bryant Z and Smith S B 2003 *Nature* **421** 423
[2] Marko J F and Siggia E D 1994 *Science* **265** 1599
Marko J F and Siggia E D 1995 *Phys. Rev.* E **52** 5912
[3] Călugăreanu G 1959 *Rev. Roum. Math. Pure.* A **4** 5
[4] Moroz J D and Nelson P 1997 *Proc. Natl. Acad. Sci. USA* **94** 14418
Moroz J D and Nelson P 1998 *Macromolecules* **31** 6333
[5] Bouchiat C and Mezard M 1998 *Phys. Rev. Lett.* **80** 1556
Bouchiat C and Mezard M 2000 *Eur. Phys. J.* E **2** 377
[6] Maritan A, Micheletti C, Trovato A and Banavar J R 2000 *Nature* **406** 287
[7] Banavar J R, Maritan A, Micheletti C and Trovato A 2002 *Proteins* **47** 315
[8] Banavar J R, Flammini A, Marenduzzo D, Maritan A and Trovato A 2003 *ComPlexUs* **1** 4
[9] Hoang T X, Trovato A, Seno F, Banavar J R and Maritan A 2004 *Proc. Natl. Acad. Sci. USA* **101** 7960
[10] Buck G and Orloff J 1995 *Topol. Appl.* **61** 205–14
[11] Gonzalez O and Maddocks J 1999 *Proc. Natl Acad. Sci. USA* **96** 4769
[12] Banavar J R, Gonzalez O, Maddocks J H and Maritan A 2003 *J. Stat. Phys.* **110** 35
[13] Banavar J R and Maritan A 2003 *Rev. Mod. Phys.* **75** 23
[14] Katrich V, Olson W K, Pieranski P, Dubochet J and Stasiak A 1997 *Nature* **388** 148–51
[15] Marenduzzo D and Micheletti C 2003 *J. Mol. Biol.* **330** 485
[16] Panyukov S and Rabin Y 2000 *Phys. Rev. Lett.* **85** 2404
Panyukov S and Rabin Y 2000 *Phys. Rev.* E **62** 7135
[17] Kamien R D 2002 *Rev. Mod. Phys.* **74** 953
[18] Gonzales O, Maddocks J H, Schuricht F and von der Mosel H 2002 *Calc. Var.* **14** 29
[19] Freed K F 1971 *J. Chem. Phys.* **54** 1453